Monthly Notices of the ROYAL ASTRONOMICAL SOCIETY

MNRAS **461,** 4246–4255 (2016) doi:10.1093/mnras/stw1633
Advance Access publication 2016 July 7

Chemical separation of disc components using RAVE

Jennifer Wojno,[1⋆] Georges Kordopatis,[1⋆] Matthias Steinmetz,[1⋆] Paul McMillan,[2] Gal Matijevič,[1] James Binney,[3] Rosemary F. G. Wyse,[4] Corrado Boeche,[5] Andreas Just,[5] Eva K. Grebel,[5] Arnaud Siebert,[6] Olivier Bienaymé,[6] Brad K. Gibson,[7] Tomaž Zwitter,[8] Joss Bland-Hawthorn,[9] Julio F. Navarro,[10†] Quentin A. Parker,[11] Warren Reid,[12,13] George Seabroke[14] and Fred Watson[15]

[1]*Leibniz Institut für Astrophysik Potsdam, An der Sternwarte 16, D-14482 Potsdam, Germany*
[2]*Lund Observatory, Lund University, Department of Astronomy and Theoretical Physics, Box 43, SE-22100 Lund, Sweden*
[3]*Rudolf Peierls Centre for Theoretical Physics, Keble Road, Oxford OX1 3NP, UK*
[4]*Department of Physics and Astronomy, Johns Hopkins University, 3400 N. Charles St, Baltimore, MD 21218, USA*
[5]*Astronomisches Rechen-Institut, Zentrum für Astronomie der Universität Heidelberg, Mönchhofstr. 12–14, D-69120 Heidelberg, Germany*
[6]*Observatoire astronomique de Strasbourg, Université de Strasbourg, CNRS, UMR 7550, 11 rue de l'Université, F-67000 Strasbourg, France*
[7]*E.A. Milne Centre for Astrophysics, University of Hull, Hull HU6 7RX, UK*
[8]*Faculty of Mathematics and Physics, University of Ljubljana, 1000 Ljubljana, Slovenia*
[9]*Sydney Institute for Astronomy, School of Physics A28, University of Sydney, NSW 2006, Australia*
[10]*Department of Physics and Astronomy, University of Victoria, Victoria, BC V8P 5C2, Canada*
[11]*Department of Physics, Chong Yuet Ming Physics Building, The University of Hong Kong, Pokfulam, Hong Kong*
[12]*Department of Physics and Astronomy, Macquarie University, Sydney, NSW 2109, Australia*
[13]*Western Sydney University, Locked Bag 1797, Penrith South DC, NSW 1797, Australia*
[14]*Mullard Space Science Laboratory, University College London, Holmbury St Mary, Dorking, RH5 6NT, UK*
[15]*Australian Astronomical Observatory, North Ryde, NSW 2113, Australia*

Accepted 2016 July 5. Received 2016 July 5; in original form 2016 March 25

ABSTRACT

We present evidence from the RAdial Velocity Experiment (RAVE) survey of chemically separated, kinematically distinct disc components in the solar neighbourhood. We apply probabilistic chemical selection criteria to separate our sample into α-low ('thin disc') and α-high ('thick disc') sequences. Using newly derived distances, which will be utilized in the upcoming RAVE DR5, we explore the kinematic trends as a function of metallicity for each of the disc components. For our α-low disc, we find a negative trend in the mean rotational velocity (V_ϕ) as a function of iron abundance ([Fe/H]). We measure a positive gradient $\partial V_\phi/\partial$[Fe/H] for the α-high disc, consistent with results from high-resolution surveys. We also find differences between the α-low and α-high discs in all three components of velocity dispersion. We discuss the implications of an α-low, metal-rich population originating from the inner Galaxy, where the orbits of these stars have been significantly altered by radial mixing mechanisms in order to bring them into the solar neighbourhood. The probabilistic separation we propose can be extended to other data sets for which the accuracy in [α/Fe] is not sufficient to disentangle the chemical disc components a priori. For such data sets which will also have significant overlap with *Gaia* DR1, we can therefore make full use of the improved parallax and proper motion data as it becomes available to investigate kinematic trends in these chemical disc components.

Key words: Galaxy: abundances – Galaxy: disc – Galaxy: evolution – Galaxy: kinematics and dynamics – Galaxy: structure.

1 INTRODUCTION

In recent years, the study of the history of our Galaxy through detailed observations of stellar populations has developed into the field known as Galactic archaeology. From our position within the Milky Way, we have the unique opportunity to study stellar dynamics and chemistry in great detail. Large-scale spectroscopic surveys such as RAdial Velocity Experiment (RAVE; Steinmetz et al. 2006), SEGUE (Yanny et al. 2009), APOGEE (Majewski et al. 2015), *Gaia*-ESO (Gilmore et al. 2012), LAMOST (Zhao et al. 2012), and GALAH (De Silva et al. 2015) now make it possible to disentangle the history of star formation and chemical

⋆ E-mail: jwojno@aip.de (JW); gkordopatis@aip.de (GK); msteinmetz@aip.de (MS)
† Senior CIFAR Fellow.

enrichment, and thus to reconstruct the development of the Galaxy as a whole.

Stars hold chemical information about their birth environment in the composition of their atmospheres, which remain relatively constant over their main-sequence lifetime (Freeman & Bland-Hawthorn 2002). If stars remained at their birth radii throughout their entire lives, and the metallicity of the interstellar medium (ISM) increased monotonically, we would expect to observe a tight correlation between stellar metallicity and age; however, in the solar neighbourhood, a range of metallicities have been observed at a given age (e.g. Edvardsson et al. 1993; Haywood 2008; Bergemann et al. 2014). For the oldest stars ($\tau > 8$ Gyr), a correlation between age and metallicity *is* observed (Haywood et al. 2013), and a variety of mechanisms have been proposed to reconcile the lack of correlation for stars younger than 8 Gyr. The mechanisms include a non-monotonic increase in metallicity (e.g. inhomogeneities in the early turbulent ISM; Brook et al. 2004; Bournaud, Elmegreen & Martig 2009; Haywood et al. 2013), and dynamics of stars such that they are sometimes observed far from their birth radii.

Sellwood & Binney (2002) discussed the impact of orbital dynamics on age–metallicity relations in terms of two processes. As a star ages, the eccentricity of its orbit increases, widening the radial band within which the star may be observed. This process they called 'blurring'. Sellwood & Binney (2002) showed that from time to time a star's guiding centre can shift fairly abruptly to a smaller or larger radius following an interaction with a transient non-axisymmetric perturbation of the disc. They dubbed this process 'churning'. Whereas blurring on its own is not powerful enough to account for the wide range of metallicities present near the Sun at a given age, Schönrich & Binney (2009b) argued that churning and blurring working together account rather nicely for the data from the Geneva–Copenhagen Survey (Nordström et al. 2004; Holmberg, Nordström & Andersen 2007).

Of particular interest in the context of radial mixing are stars with super-solar metallicity, or super-metal-rich (SMR)[1] stars (Kordopatis et al. 2015a). The presence of these metal-rich stars in the solar neighbourhood has long been problematic for the theory of Galactic chemodynamics (e.g. Grenon 1972; Israelian & Meynet 2008). The ISM in the solar neighbourhood is expected now to be as metal-rich as it has ever been, and is now around solar metallicity and relatively homogeneous (Cartledge et al. 2006). If we assume a monotonic metallicity gradient in the disc, for SMR stars we infer birth radii $R \lesssim 3$ kpc (Kordopatis et al. 2015a).

For lower metallicities, we consider the chemodynamical history of the thick disc. While the mechanisms by which the thick disc formed are hotly debated, the thick disc consists mostly of old, metal-poor ($\sim -1.5 <$ [Fe/H] < 0.1), α-enhanced stars on kinematically hotter orbits than thin disc stars (Chiba & Beers 2000; Bensby, Feltzing & Lundström 2003). Although Bovy, Rix & Hogg (2012a), using low-resolution spectra, argued that the thin and the thick discs blend continuously into one another, a trough in the density of stars in the space of α-abundance versus metallicity leads the majority of authors to suppose that the thin and thick discs have experienced different evolutionary histories (e.g. Fuhrmann 2011; Lee et al. 2011; Adibekyan et al. 2013; Haywood et al. 2013; Bensby, Feltzing & Oey 2014; Recio-Blanco et al. 2014; Guiglion et al. 2015; Hayden et al. 2015; Kordopatis et al. 2015b). Indeed, Aumer, Binney & Schönrich (2016) show that in *N*-body models scattering of stars by the inevitable non-axisymmetric features in a disc generates structures remarkably like the thin disc, but does not generate significant thick discs (see also Minchev et al. 2012, but also Schönrich & Binney 2009a,b; Loebman et al. 2011 for how thick discs may be formed due to radial migration). They conclude that the thick disc was present before the thin disc started to form. By assigning stars as belonging to either the thin or thick disc according to their chemical properties, we can explore the possible differences in the chemodynamical properties of these populations.

In this paper, we aim to identify chemically distinct thin and thick disc components using the medium-resolution ($R \sim 7500$) RAVE survey (Steinmetz et al. 2006). The magnitude-limited ($9 < I < 12$) RAVE survey offers a kinematically unbiased sample of stars, ideal for investigating stellar dynamics. The fourth data release (DR4), presented in Kordopatis et al. (2013, hereafter K13), provides radial velocities, stellar parameters, abundance measurements (Boeche et al. 2011), and distance estimates (Binney et al. 2014a) for 425 561 stars, making it one of the largest spectroscopic surveys with unique statistical strengths. Combining these radial velocity data and distance estimates with proper motions, full 6D (position and velocity) information is available for the majority of stars.

The paper is organized as follows: Section 2 briefly describes the quality criteria and parameter cuts applied to obtain the final working sample, improvements on the data set, and methods to derive stellar kinematic properties used in the analysis. Section 3 describes the method used to disentangle the chemical disc components. Section 4 presents the kinematic trends for each component. We characterize the trends in mean V_ϕ velocity for both the α-low and α-high populations, and discuss trends observed in the dispersions of all three velocity components. We also estimate the scalelengths of our chemically selected discs. In Section 5, we discuss implications for these findings, and in particular discuss possible origins of our metal-rich, α-low stars. Finally, Section 6 summarizes our results.

2 RAVE DATA SAMPLE AND KINEMATICS

To ensure a high-quality sample of stars in the extended solar neighbourhood, we use a subsample of RAVE DR4 that meets a number of quality criteria. First, we select stars with signal-to-noise per pixel >80. We remove stars that emerge from the chemical abundance pipeline (Boeche et al. 2011) with CHISQ_c > 2000, so retaining only stars with a good fit between template and observed spectra. In addition, we require the quality flag on the convergence of the DR4 pipeline to be Algo_Conv_K $\neq 1$.[2] Finally, we utilize stellar classification flags described in Matijevič et al. (2012) to exclude a small fraction of stars with spectra for which the learning grid contains no template – e.g. stars with chromospheric emission (Žerjal et al. 2013), spectra with wavelength calibration problems, carbon stars, and binary stars.

After these quality cuts have been applied, we remove all stars with line-of-sight distances greater than 1 kpc. We focus our investigation on the kinematics of stars in the extended solar neighbourhood because the global properties in this domain have been extensively studied, and the metallicity gradient $\partial[M/\mathrm{H}]/\partial R \sim -0.06\,\mathrm{km\,s^{-1}\,kpc^{-1}}$ (e.g. Boeche et al. 2013; Genovali et al. 2014) and velocity gradient $\partial V_{R,\phi,Z}/\partial R \sim \pm 3\,\mathrm{km\,s^{-1}\,kpc^{-1}}$ (e.g. Siebert et al. 2011; Monari et al. 2014) are

[1] For our sample, we define SMR stars as those with [Fe/H] $\gtrsim 0.15$.

[2] A flag of 1 indicates that the pipeline failed to converge (for more details see K13).

such that changes in mean velocity and metallicity across this volume are small. In addition, we require that the total space velocity, $V_{\rm tot}$, is less than the Galactic escape speed, $V_{\rm esc}$, where we adopt the lower limit $V_{\rm esc} \geq 492\,{\rm km\,s^{-1}}$ determined by Piffl et al. (2014). Our sample is further reduced because not all RAVE stars have abundance measurements in DR4. After these cuts, we are left with a sample of 20 751 stars, which is evenly split between 10 384 dwarfs and 10 367 giants.

Galactocentric space velocities in a right-handed cylindrical coordinate system were determined using the equations summarized in appendix A of Williams et al. (2013). First, to transform the observed velocities into a Galactocentric coordinate system, we adopt values for the solar peculiar motion with respect to the local standard of rest (LSR) of $(U, V, W)_\odot = (11.10, 12.24, 7.25)$ km s^{-1} from Schönrich, Binney & Dehnen (2010). In addition, we take the location of the Sun to be $(R_0, z_0) = (8.3, 0)$ kpc and the LSR speed to be $V_{\rm LSR} \sim 240$ km s^{-1} (Schönrich 2012). When calculating the Galactocentric space velocities, we use radial velocity measurements from DR4, Galactic coordinates (ℓ, b) from 2MASS (Skrutskie et al. 2006), and proper motion measurements from UCAC4 (Zacharias et al. 2013).[3] Distances have been provided using a version of the RAVE distance pipeline (Binney et al. 2014a) that has been updated to include an extended range of Padova isochrones (Bertelli et al. 2008) down to [Fe/H] $= -2.2$, while it was previously limited to -0.9 dex. These improved distances only systematically affect the results for the most metal-poor stars.

3 CHEMICAL SEPARATION OF THE DISC

We separate our sample into two populations using a chemical criterion: the star's position in plane spanned by α-abundance ([Mg/Fe]) versus iron abundance ([Fe/H]). While the thin (D) and thick disc (TD) overlap spatially and kinematically, several studies have shown that it is possible to disentangle the two components in the [α/Fe]–[Fe/H] plane. These studies include surveys of nearby stars (Fuhrmann 1998, 2004, 2008, 2011), a low-resolution study of extended solar neighbourhood G-dwarfs (Lee et al. 2011), and a number of recent high-resolution studies (Reddy, Lambert & Allende Prieto 2006; Adibekyan et al. 2013; Haywood et al. 2013; Bensby et al. 2014; Recio-Blanco et al. 2014; Guiglion et al. 2015; Hayden et al. 2015; Kordopatis et al. 2015b). RAVE DR4 provides abundance measurements for six elements derived from the RAVE chemical pipeline, which includes the α elements Mg, Si, and Ti. K13 suggested that Ti is not reliably measured for dwarfs, and dwarfs make up half our sample, so we use the Mg abundance measurement only.

The precision of [Mg/Fe] abundances determined with RAVE ($\sim$0.2 dex) is lower than that required to recover the gap between the two populations in the [α/Fe]–[Fe/H] plane: using equation 3 of Lindegren & Feltzing (2013), which describes the minimum separation at which two populations can be distinguished in a given sample size, we find that with our sample of 20 751 stars we could distinguish populations separated by 1.5 times the standard error in [Mg/Fe]. Hence, given our error of $\sim$0.2 dex in [Mg/Fe], the separation between populations needs to be at least 0.3 dex, whereas high-resolution data indicate that the separation is $\lesssim$0.2 dex (Haywood et al. 2013; Bensby et al. 2014; Recio-Blanco et al. 2014; Kordopatis et al. 2015b). Therefore, we turn to a probabilistic approach to the separation of the α-low and α-high stars.

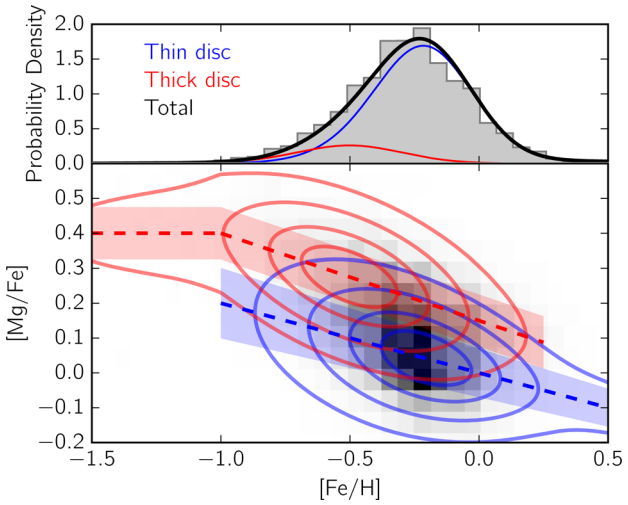

Figure 1. Top panel: adopted MDF. The grey shaded histogram represents the MDF of our final sample. The thin and thick disc MDFs are shown in blue and red, respectively, and the thick black line is the sum of both disc components. Bottom panel: 2D histogram of our sample in [Mg/Fe]–[Fe/H] space. Contours show 33, 67, 90, and 99 per cent of thin disc (blue) and thick disc (pink) 2D pdfs. The overplotted dashed blue line shows the assumed mean ($\mu_{\rm Mg}$) variation as a function of [Fe/H], where the filled area represents the assumed variation in the $\sigma_{\rm Mg}$ as a function of [Fe/H], for the thin disc (equations 3 and 4). Similarly, the overplotted dashed red line shows the adopted thick disc relations (equations 5 and 6).

We write the 2D probability density function (pdf) of stars in the α-low or the α-high component as

$$f([{\rm Fe/H}], [\alpha/{\rm Fe}]) = f_{[{\rm Mg/Fe}]} \times f_{[{\rm Fe/H}]}. \quad (1)$$

We will refer to $f_{[{\rm Mg/Fe}]}$ as the α distribution function, and $f_{[{\rm Fe/H}]}$ as the metallicity distribution function (MDF) for a given component. The α distribution is taken to be a Gaussian with a mean and dispersion that depends on [Fe/H]:

$$f_{[{\rm Mg/Fe}]} = \frac{1}{\sigma_{\rm Mg}\sqrt{2\pi}} \exp\left(-\frac{([{\rm Mg/Fe}] - \mu_{\rm Mg})^2}{2{\sigma_{\rm Mg}}^2}\right). \quad (2)$$

For the thin disc, $\mu_{\rm Mg}$ and $\sigma_{\rm Mg}$ are given by (Kordopatis et al. 2015b)

$$\mu_{\rm Mg,D} = -0.2 \times [{\rm Fe/H}] \quad (3)$$

$$\sigma_{\rm Mg,D} = -0.031 \times [{\rm Fe/H}] + 0.07. \quad (4)$$

For the thick disc, $\mu_{\rm Mg}$ and $\sigma_{\rm Mg}$ are given by

$$\mu_{\rm Mg,TD} = \begin{cases} 0.4 & \text{for } [{\rm Fe/H}] < -1.0 \\ -0.25 \times [{\rm Fe/H}] + 0.15 & \text{otherwise} \end{cases} \quad (5)$$

$$\sigma_{\rm Mg,TD} = 0.075. \quad (6)$$

In the lower panel of Fig. 1, the linear dependences of $\mu_{\rm Mg}$ on [Fe/H] are shown by the dashed lines (blue for the α-low and red for the α-high component), while the widths of the blue and red shaded regions around these lines indicate the values of $\sigma_{\rm Mg}$ for both the α-low and -high components.

[3] While DR4 also provides a number of sources for proper motion measurements, we find no substantial difference in our results between two of the most recent catalogues (UCAC4 and PPMXL; Roeser, Demleitner & Schilbach 2010). We chose to use UCAC4 values, as this catalogue is less affected by potential systematic uncertainties (Vickers, Roeser & Grebel 2016).

Table 1. Parameters for equation (7) for both thin (D) and thick (TD) disc components.

	D	TD
a_1	0.8	0.9
$\mu_{\mathrm{Fe},1}$	−0.2	−0.5
$\sigma_{\mathrm{Fe},1}$	0.18	0.2
a_2	0.15	0.08
$\mu_{\mathrm{Fe},2}$	−0.4	−0.8
$\sigma_{\mathrm{Fe},2}$	0.2	0.4
a_3	0.05	–
$\mu_{\mathrm{Fe},3}$	0.2	–
$\sigma_{\mathrm{Fe},3}$	0.5	–
X	0.85	0.14

The MDFs are too skew to be satisfactorily represented by a single Gaussian, so we represent them as weighted sums of multiple Gaussians,

$$f_{[\mathrm{Fe/H}]} = \sum_{i=1}^{n} \frac{a_i}{\sigma_{\mathrm{Fe},i}\sqrt{2\pi}} \exp\left(-\frac{([\mathrm{Fe/H}]-\mu_{\mathrm{Fe},i})^2}{2{\sigma_{\mathrm{Fe},i}}^2}\right), \quad (7)$$

where $n = 3$ for the thin disc and $n = 2$ for the thick disc. The means, dispersions, and weights a_i of these Gaussians for both the thin and thick disc can be found in Table 1. These values were extracted using the high-resolution measurements of Kordopatis et al. (2015b) as a starting point, but the shapes of the distribution were slightly modified because the shape of the MDF in any survey is affected by the survey's selection function. The top panel of Fig. 1 shows the adopted model MDF, using the values from Table 1. We do not consider a metal-rich tail for the thick disc due to ambiguity regarding the mixture of populations in the α-high, metal-rich region of the [α/Fe]–[Fe/H] plane (more details regarding potential complications due to α-high, metal-rich stars can be found later in this section as well as in Section 6).

The pdfs given by equation (1) are normalized to unity. Since there are believed to be more stars in the thin disc than the thick disc (Bland-Hawthorn & Gerhard 2016), we multiply these normalized pdfs by factors X_{TD} and X_{D} equal to the probabilities that a randomly chosen star in the sample belongs to the thick or thin disc. The values of X_{TD} and X_{D} are not accurately known. RAVE is kinematically unbiased, and as a magnitude-limited survey that extends much further than one thin disc scaleheight, we expect thin and thick disc stars to enter the survey roughly in proportion to the local surface densities of the two discs. Our adopted values are based on the results of Soubiran, Bienaymé & Siebert (2003), who separated the thin and thick disc populations in velocity–metallicity space. They give an estimate of 15 ± 7 per cent for the local normalization of the thick disc and 85 ± 7 per cent for the thin disc, where the median distance of their sample is 400 pc from the Galactic plane. The median distance of our sample is similar, so we find it appropriate to adopt these values, modifying them slightly. We use $X_{\mathrm{TD}} = 0.14$ and $X_{\mathrm{D}} = 0.85$ (see Table 1).[4] Thus, we assume that ∼1 per cent of the stars in the extended solar neighbourhood belong to the halo. We do not explicitly calculate the probability of a star belonging to the halo, however. Chen et al. (2001) note the degeneracy between local normalization and surface density ratio due to the uncertain nature of the scaleheights of the discs. However, our chosen value is also a conservative estimate when considering the overall relative thin/thick disc surface density ratio (see Bland-Hawthorn & Gerhard 2016).

In order to include realistic errors for our [Fe/H] and [Mg/Fe] measurements (of the order of 0.17 and 0.2 dex, respectively), we generate 500 realizations of each star assuming a Gaussian error distribution for both measurements. The ratio of the thick disc probability to the thin disc probability ($f_{\mathrm{TD}}/f_{\mathrm{D}}$) is calculated for each realization, and the median is taken as the final $f_{\mathrm{TD}}/f_{\mathrm{D}}$ value. We assign a star as belonging to the thin disc when $f_{\mathrm{TD}}/f_{\mathrm{D}} < 0.1$. Similarly, we assign a star as belonging to the thick disc when $f_{\mathrm{TD}}/f_{\mathrm{D}} > 10$. We note that we still expect some overall contamination of incorrectly assigned stars in both disc components, of the order of 10 per cent, due to our selection criterion ($f_{\mathrm{TD}}/f_{\mathrm{D}}$), and this contamination increases towards both ends of our metallicity distribution. This contamination may have a number of sources. Stars may be incorrectly assigned to the thick disc due to the substantial overlap in the MDF of the thin and thick disc at the metal-rich end. In addition, the precision of our abundance measurements may affect the assignment accuracy at both tails of the distribution.

Despite this contamination, we consider that the α-low component corresponds to what would typically be described as the 'thin disc', and the α-high similarly corresponds to the 'thick disc'. In the remainder, we refer to the 'thin disc' as the α-low component and the 'thick disc' as the α-high component. We adopt this definition due to certain limitations when considering the tails of [Fe/H] distribution for both the 'thin' and 'thick' disc components, where more complex population mixtures may exist (Nissen & Schuster 2010; Chiappini et al. 2015; Martig et al. 2015; Masseron & Gilmore 2015). Specifically, for the metal-rich tail of the α-high component, it is unclear if the distribution flattens (e.g. Bensby et al. 2014), or continues with a linear trend similar to our adopted distribution, eventually joining the α-low sequence. In either case, disentangling these complex population mixtures in the metal-rich tail is not possible when considering the precision of our α-abundance measurements, and therefore we consider only a conservative range of metallicities where a two-component model is viable.

Our final sample consists of 11 440 stars assigned to the α-low component and 2251 stars assigned to the α-high component. In Fig. 2, we show [Mg/Fe] versus [Fe/H], with bins colour-coded according to the average probability of stars in that bin to belong to either component. The contours enclose 33, 67, 90, and 99 per cent of the selected α-low (blue) and α-high (pink) components, to illustrate the gap between the two components.

4 RESULTS

Each pixel of the [Fe/H]–[Mg/Fe] planes of Fig. 3 is coloured to encode the mean value of V_R, V_ϕ, or V_Z for the stars in our selection that are assigned to that pixel. A clear distinction is evident between the kinematics of our selected α-low and α-high components, especially in V_ϕ.

To explore further the different kinematic trends in our chemical components, in Fig. 4 we show for each component the averages of V_R, V_ϕ, and V_Z as a function of metallicity. In the case of V_ϕ, we have fitted by least-squares lines to the data points, excluding bins with less than 10 objects to avoid drawing conclusions from low-number statistics. For the α-low sequence, the most metal-poor bins are also excluded as there we expect some contamination from the α-high component (see Section 3). For the α-high disc (bottom row of Fig. 4), we exclude the two most metal-rich bins, due to

[4] As these values are widely disputed, we explore the effects of removing the X_{TD} and X_{D} factors from our probability computations (i.e. giving both disc components equal weight). The corresponding results can be found in Sections 4.1 and 4.2.

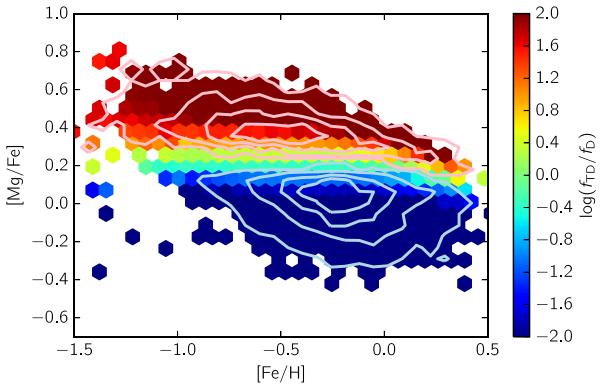

Figure 2. [Mg/Fe] versus [Fe/H], where the colour of the bins represents the logarithm $\log_{10}(f_{\rm TD}/f_{\rm D})$ of the average relative probability of stars in that bin belonging to either the thick or the thin disc. Stars with a relative probability between 0.1 and 10 are not subsequently used but are included here to demonstrate the gradient in probability. The contours show 33, 67, 90, and 99 per cent of the selected thin disc (blue) and thick disc (pink) distributions, to illustrate the gap between the two components.

contamination from α-low stars. Bins excluded from the linear fits are plotted as open circles.

4.1 Mean rotational velocity trends for the thin and thick disc components

We find $\partial V_\phi/\partial[{\rm Fe/H}] < 0$ for the α-low component but $\partial V_\phi/\partial[{\rm Fe/H}] > 0$ for the α-high component. Quantitatively, for α-low stars, we find

$$\frac{\partial V_\phi}{\partial[{\rm Fe/H}]} = (-11 \pm 1)\,{\rm km\,s^{-1}\,dex^{-1}}. \quad (8)$$

This slope is significantly shallower than those of Lee et al. (2011) and Adibekyan et al. (2013), but using high-resolution data from *Gaia*-ESO Recio-Blanco et al. (2014) find $\partial V_\phi/\partial[M/{\rm H}] = (-17 \pm 6)\,{\rm km\,s^{-1}\,dex^{-1}}$, which lies within 1σ of our value.

For the α-high population, we measure

$$\frac{\partial V_\phi}{\partial[{\rm Fe/H}]} = (51 \pm 10)\,{\rm km\,s^{-1}\,dex^{-1}}. \quad (9)$$

This slope is in agreement with recent literature values. Lee et al. (2011) report a tight correlation with slope $(43.4 \pm 1.8)\,{\rm km\,s^{-1}\,dex^{-1}}$ in their subsample of thick disc G-dwarfs, while Kordopatis et al. (2011) find $\partial V_\phi/\partial[M/{\rm H}] = (43 \pm 11)\,{\rm km\,s^{-1}\,dex^{-1}}$. Similarly, Adibekyan et al. (2013) find $\partial V_\phi/\partial[M/{\rm H}] \sim 42\,{\rm km\,s^{-1}\,dex^{-1}}$ for thick disc stars in a sample of FGK solar neighbourhood dwarfs. Our value also agrees with the findings of Recio-Blanco et al. (2014), $\partial V_\phi/\partial[M/{\rm H}] = (43 \pm 13)\,{\rm km\,s^{-1}\,dex^{-1}}$, from a high-resolution sample of FGK stars from the *Gaia*-ESO survey.

Fig. 5 shows the average V_ϕ velocity as a function of [Fe/H] for the case where both discs are given equal weight (compare with panels c and d of Fig. 4). We measure similar trends in $\partial V_\phi/\partial[{\rm Fe/H}]$ as when the $X_{\rm TD}/X_{\rm D}$ prior is included, for both disc components. This further strengthens our result that we successfully determine distinct kinematics for each disc component.

4.2 Velocity dispersion trends

Fig. 6 shows for the α-low and α-high components the variation with [Fe/H] of the dispersions of V_R, V_ϕ, and V_Z corrected for observational uncertainties in the standard way:

$$\sigma_{R,\phi,Z} = \sqrt{\sigma^{*2}_{R,\phi,Z} - \langle {\rm e}_{V_{R,\phi,Z}} \rangle^2}, \quad (10)$$

where $\sigma_{R,\phi,Z}$ is our corrected velocity dispersion, $\sigma^*_{R,\phi,Z}$ is the measured velocity dispersion, and ${\rm e}_{V_{R,\phi,Z}}$ is the error on the velocity component. In both chemical subgroups, velocity dispersion tends to decrease with increasing [Fe/H], so the most metal-poor stars have the highest dispersions and SMR stars have low dispersions. In the region $-0.2 < [{\rm Fe/H}] < 0.0$, the trends for the α-low and α-high components overlap substantially: their dispersions differ little in the two overlapping bins where both the α-low and α-high components are free of significant contamination. However, at $[{\rm Fe/H}] < -0.2$ the values for each chemical subgroup are clearly separated. While we assume some contamination of the α-low sample in the most metal-poor bins, these bins follow approximately the same linear relation as the more metal-rich bins. We find the ratio of σ_R/σ_ϕ to be relatively constant ($\sim$1.6 for both components), independent of metallicity.

At the top right of each panel in Fig. 6, we give the mean velocity dispersion for each chemical component, calculated using only the bins that we consider free of significant contamination (i.e. avoiding the two most metal-poor bins for the α-low component, and the two most metal-rich bins for the α-high component). This gives an effective range of $-0.27 < [{\rm Fe/H}] < 0.38$ for the α-low component, and an effective range of $-1.15 < [{\rm Fe/H}] < -0.05$ for the α-high component.

For both components, our mean velocity dispersions conform to the familiar relations $\sigma_R > \sigma_\phi > \sigma_Z$ and $\sigma_Z \simeq 0.5\sigma_R$ (Quillen & Garnett 2001; Holmberg et al. 2007). In addition, we find a constant offset $\sim$16 km s^{-1} between the average dispersions of the α-low

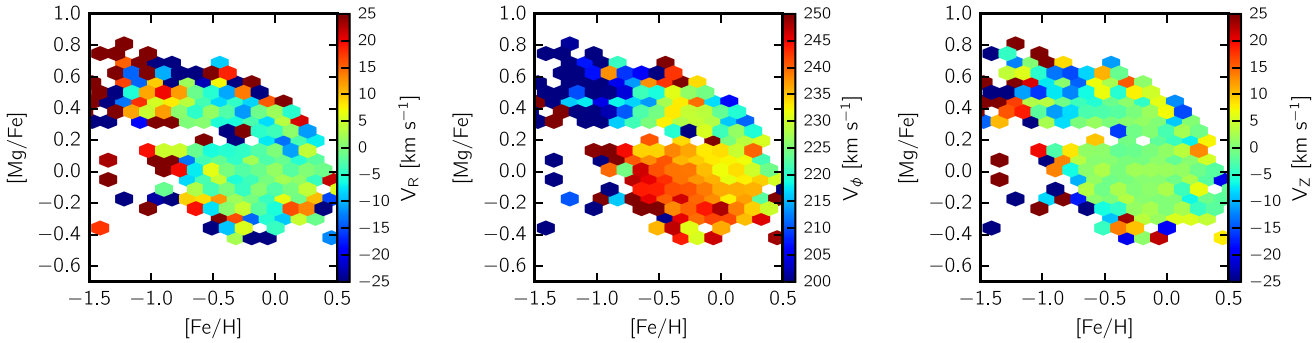

Figure 3. [Mg/Fe] versus [Fe/H], where the colour of the bins represents the average velocity of the stars in that bin, for each of the three velocity components. Here, we show only the selected stars, i.e. all stars with $0.1 < (f_{\rm TD}/f_{\rm D}) < 10$ have been removed.

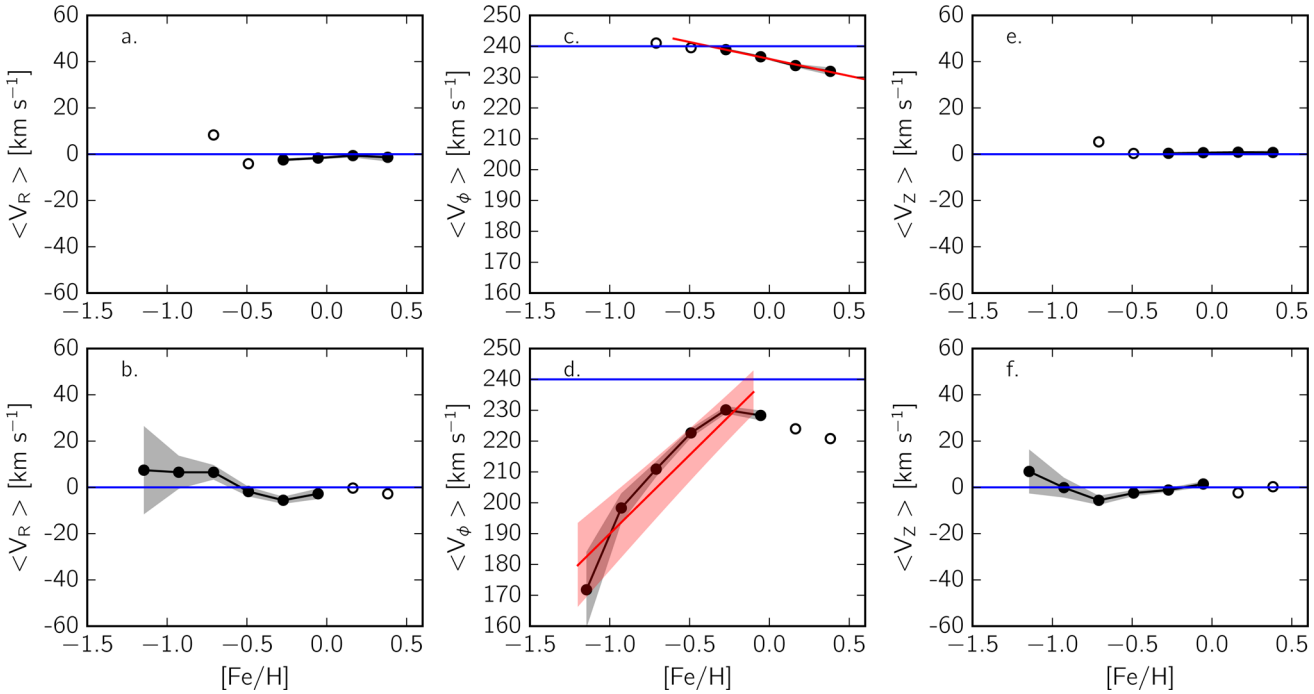

Figure 4. Mean velocity as a function of [Fe/H] for the α-low component (top row), and the α-high component (bottom row). See Section 3 for a detailed description on how these populations are selected. Trend lines are computed by binning the data into ∼0.2 dex wide [Fe/H] bins. The shaded regions correspond to the average errors for a given metallicity bin. Bins with less than 10 stars are not shown, and are not used to calculate the linear fit. Open circles denote bins which are not used in determining the linear fit in panels c and d. The red lines in panels c and d show the linear fits for the α-low and -high sequences, respectively, with the red shaded region corresponding to the error on the fit.

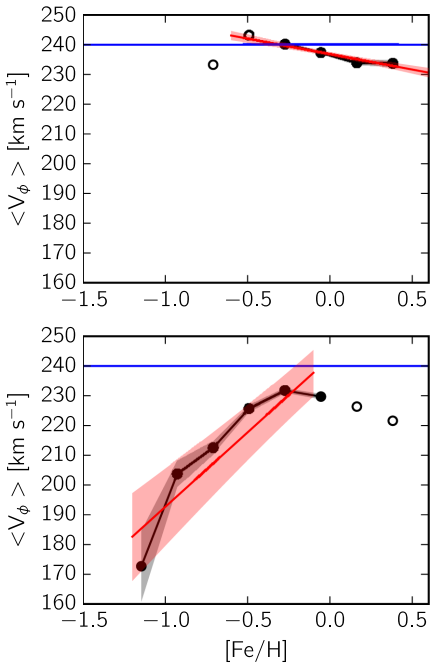

Figure 5. Same as panels c and d of Fig. 4, but with no prior factors used in the determination of the probabilities (i.e. equal weight given to both disc components, cf. to the $X_{\rm TD}$ and $X_{\rm D}$ factors given in Table 1).

and α-high sequences. This offset is consistent with the observed values of Bensby et al. (2005), which were determined using a kinematically selected high-resolution sample of FGK dwarfs in the solar neighbourhood. As in Section 4.1, we consider the velocity dispersion as a function of [Fe/H] for the case where we remove the $X_{\rm TD}/X_{\rm D}$ prior from the probability calculation. The results are shown in Fig. 7. While the outcome is similar, we do note that the thick disc has a consistently lower mean velocity dispersion compared to the case where we include the prior. In addition, the separation between the two chemical disc components is also consistently less (∼13 km s^{-1} compared to when the prior is included ∼16 km s^{-1}, cf. Figs 6 and 7).

While the removal of the $X_{\rm TD}/X_{\rm D}$ factor does not significantly alter our results, the ratio of stars assigned to the α-high and -low components is affected adversely. The ratio of α-high to α-low stars for our final selected sample is 2251/11 440 ∼ 0.20, which is within the range of conservative estimates of the thick disc fraction. In contrast, if we remove the prior, we find a ratio of 4436/7785 ∼ 0.60, which is above the high end of the range of estimates. In order to better represent physical reality as it is currently understood, we find the application of this prior desirable.

Combining the mean and dispersion of each of velocity component with the Jeans equation, we can estimate the radial scalelengths (h_R) of our chemical disc components. If we assume that the Galactic potential is dominated by a centrally concentrated mass distribution (Gilmore, Wyse & Kuijken 1989), and that the velocity ellipsoid always points towards the Galactic Centre (Siebert et al. 2008; Pasetto et al. 2012; Binney et al. 2014b), we have

$$h_R = \frac{2R\sigma_R^2}{V_c^2 - \langle V_\phi \rangle^2 + 2\sigma_R^2 - \sigma_\phi^2 - \sigma_Z^2} \quad . \tag{11}$$

By this reckoning our α-low component has scalelength $h_{R_{\rm D}} = 4.8 \pm 0.2$ kpc, and our α-high component has $h_{R_{\rm TD}} = 3.4 \pm 0.1$ kpc. Our estimates are consistent with the finding of Bovy et al. (2012b) from a sample of local dwarfs from SEGUE, that the

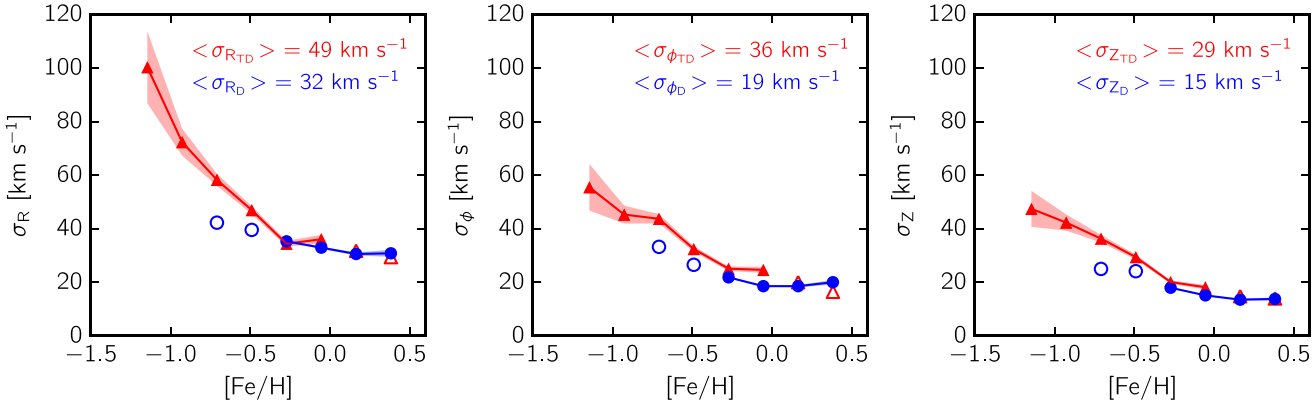

Figure 6. Velocity dispersion as a function of metallicity for the α-low component (blue circles), and the α-high component (red triangles). See Section 3 for a detailed description on how these populations are selected. Trend lines are computed by binning the data into ∼0.2 dex width bins. The shaded regions correspond to average errors for a given metallicity bin. Bins with less than 10 stars are not shown. The average $\sigma_{R,\phi,Z}$ values are given in the top-right corner, for both disc components. These averages are determined using only bins with filled symbols.

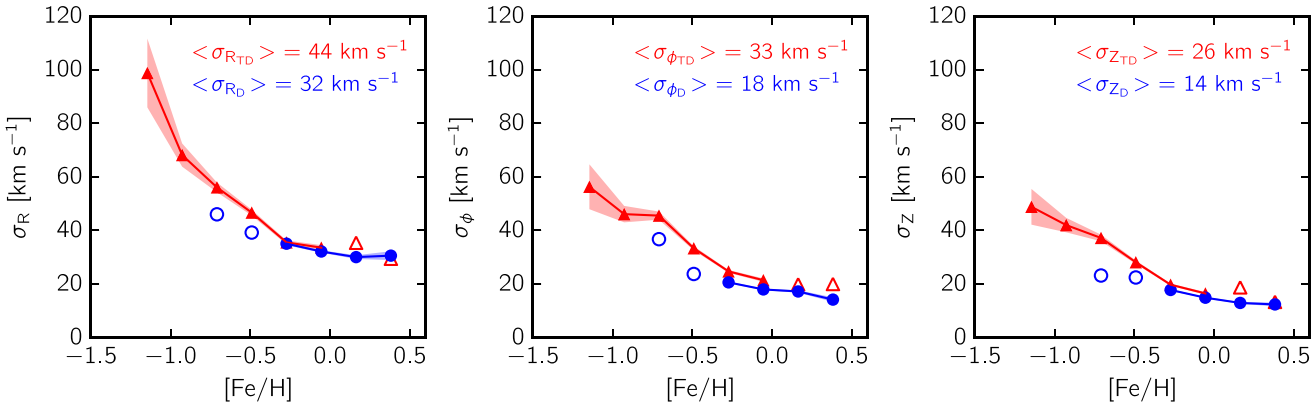

Figure 7. Same as Fig. 6, but with no prior factors used in the determination of the probabilities (i.e. equal weight given to both disc components).

scalelength of the thin disc is more extended than that of the thick disc. When we consider the scalelengths of the discs as functions of metallicity, for the α-low component $\partial h_R/\partial$[Fe/H] < 0 (i.e. the most metal-poor bins have the longest scalelengths). The scalelength of the α-high component proves relatively constant, with only a slight negative trend, with increasing metallicity.

While the scalelength of our α-low component is longer than that determined by Robin et al. (2003) and Jurić et al. (2008) from star counts, it lies within 2σ of high-end estimates, such as that, $h_R = (4.3 \pm 0.2)$ kpc, of Bovy et al. (2012b), who used a sample of dwarfs with [Fe/H] ~ 0. Our value of h_R for the α-high component is also larger than literature values. Using a handful of red giant stars, Bensby et al. (2011) obtain $h_R \sim 2$ kpc for the thick disc, and Bovy et al. (2015) find $h_R = (2.2 \pm 0.2)$ kpc for an α-high population. However, we note that the values of our scalelengths depend sensitively on the adopted value for the peculiar motion of the Sun ($V_\odot$). A smaller $V_\odot$ (e.g. the classical value of 5.25 km s^{-1}; Aumer & Binney 2009) would result in much smaller scalelengths for both discs. For a detailed discussion, see Golubov et al. (2013).

Many of the previous studies cited use either dwarfs or giants for their samples, with a tendency to select only dwarfs for chemodynamical studies, as their atmospheres stay relatively constant until they leave the main sequence. Giants, on the other hand, can experience a significant amount of mixing in their atmospheres, which makes them less desirable for studies involving long dynamical time-scales. As we have an equal number of dwarfs and giants in our original sample before the chemical disc selection, we investigated if these observed trends are affected when considering only dwarfs, or only giants. For both the mean velocity and velocity dispersion trends, we find no significant differences in our conclusions.

5 DISCUSSION

The primary difference in the kinematics of our α-low and α-high components is the trends in mean rotational velocity as a function of [Fe/H]. We find opposite signs for $\partial V_\phi/\partial$[Fe/H] for our two chemical disc components: positive for the α-high component and negative for the α-low component (see panels c and d of Fig. 4).

The α-high component exhibits the expected characteristics of asymmetric drift: as [Fe/H] and rotational velocity increase, the velocity dispersion decreases. On account of asymmetric drift, the 'thick' disc lags the LSR significantly – Bensby et al. (2005) find a lag of 46 km s^{-1} for the kinematically selected thick disc. While the value of the thick disc's lag is uncertain (cf. Chiba & Beers 2000; Fuhrmann 2004; Lee et al. 2011), positive values for $\partial V_\phi/\partial$[Fe/H] have also been observed in a number of previous studies (Kordopatis et al. 2011; Lee et al. 2011; Adibekyan et al. 2013; Recio-Blanco et al. 2014). Recio-Blanco et al. (2014) suggest that this positive trend is in agreement with the scenario described in Haywood et al. (2013, 2016): each subsequent stellar generation in the thick disc is kinematically cooler than the previous one, such

that the dispersion (and therefore lag behind the LSR) decreases with increasing [Fe/H].

Haywood et al. (2013) then propose that the inner disc is formed with the properties of the most metal-rich thick disc 'layer', with quenching of star formation causing the corresponding gap found in the [α/Fe]–[Fe/H] plane. What could have caused star formation to pause at the end of the formation of the thick disc is still debated, although a few scenarios have been proposed [e.g. the formation of the bar (Haywood et al. 2016) and depletion of gas in the disc (Chiappini, Matteucci & Gratton 1997)]. Star formation is then assumed to resume, albeit at a lower rate, in the thin disc (Just & Jahreiß 2010).

Our α-low component also lags the LSR, but with $\partial V_\phi/\partial$[Fe/H] negative. We propose that the SMR stars ([Fe/H] $\gtrsim 0.15$) in our α-low component have undergone significant changes in their orbital kinematics. The origin of these metal-rich stars is not immediately obvious, but it is likely that they did not form locally. In order to explain the presence of such stars, we consider various Galactic evolution mechanisms.

It has been suggested by Haywood et al. (2013) that a turbulent ISM (Brook et al. 2004; Bournaud et al. 2009) in the inner Galaxy could allow gas enrichment to reach solar metallicity within a few Gyr. SMR stars born in the inner Galaxy would then experience interactions with inhomogeneities in the primitive disc to bring them to the solar neighbourhood. However, Kordopatis et al. (2015a) note that stars formed in the early turbulent ISM would now be on highly eccentric orbits, which is not the case for most SMR stars in RAVE (see their figs 9 and 10). It is also possible that these stars were formed in gas clouds on non-circular orbits (e.g. from gas being accreted from outside the disc), and therefore the stars would, from birth, be on kinematically hotter orbits themselves. However, such gas is typically of sub-solar metallicity (Richter et al. 2001; Wakker 2001; Richter 2006) and therefore would most likely not give rise to the metal-rich population that we see.

Now consider the possibility that the SMR stars were born kinematically cold. If these stars were scattered on to more eccentric/inclined orbits by either the Lindblad resonances of the spiral arms or by giant molecular clouds ('blurring'), then these SMR stars in the α-low component would be visitors from the inner Galaxy at the apocentres of their orbits. On this account they would lag the LSR as we observe. We find that our most metal-rich stars ([Fe/H] $\gtrsim 0.3$) lag the LSR by $\sim$10 km s^{-1}. Golubov et al. (2013) argue that this asymmetric drift should also be reflected in increasing radial velocity dispersion, i.e. increasing σ_R with decreasing $\langle V_\phi \rangle$. For our α-low component, we find the trends of $\sigma_{R,\phi,Z}$ with [Fe/H] to be flat – Fig. 6 shows just a hint of increasing σ_R and σ_ϕ.

Although blurring may influence the relationship between chemistry, kinematics, and position that we find, we still need to explain the finding of Kordopatis et al. (2015a) that SMR stars in RAVE (defined as [Fe/H] > 0.1) follow roughly circular orbits, with approximately half of these metal-rich stars having eccentricities below $e \sim 0.15$. On the other hand, churning involves an increase in angular momentum and thus guiding radius without any increase in eccentricity. As a large fraction of these SMR stars have circular orbits, we consider it likely that these stars have been brought to the solar neighbourhood largely by churning.

A number of high-resolution studies find that the SMR stars in the α-low component have a relatively small spread in [Mg/Fe] (Haywood et al. 2013; Bensby et al. 2014; Recio-Blanco et al. 2014; Kordopatis et al. 2015b), and we find a slight indication of this at the SMR tail of our α-low component. This scenario is consistent with the model presented in Nidever et al. (2014), according to which the α-low component arises by superposition of populations with differing star formation histories. This manifests as a relatively narrow sequence of α-low stars over a large [Fe/H] range. Nidever et al. (2014) note that a possible origin of this effect is described in Schönrich & Binney (2009a), where the superposition of populations is caused by radial migration of stars from the inner Galaxy with different birth radii and enrichment histories. While they find that stars may experience both blurring and churning, the effect of churning is stronger in the inner regions of the Galaxy, where SMR stars were most likely born. Therefore, we also consider that both mechanisms may be at work. If a star is first blurred such that it is at larger Galactic radii, it is possible that it may then experience a change in guiding radius due to an interaction with a varying non-axisymmetric potential at corotation, such as transient spiral arms (Sellwood & Binney 2002), or transient overdensities at the bar–spiral interface (Minchev, Chiappini & Martig 2013). While it is possible for both mechanisms to alter the kinematics of a given star, Minchev et al. (2013) note that stars on circular orbits are more likely to be affected by churning.

6 SUMMARY AND CONCLUSIONS

We have explored the relationship between kinematics and elemental abundances for a sample of extended solar neighbourhood stars obtained by RAVE. Since high-resolution studies (e.g. Haywood et al. 2013; Bensby et al. 2014; Recio-Blanco et al. 2014; Kordopatis et al. 2015b) have shown that the trough in the [Fe/H]–[α/Fe] plane between the α-low and α-high components of the Galactic disc is narrower than the uncertainties in [α/Fe] in the RAVE survey, we have identified the RAVE stars that are most and least likely to be members of the α-low component. Specifically, a star enters our α-low sample if its location in the [Fe/H]–[α/Fe] plane is made 10 times more probable by the hypothesis that it belongs to the α-low component than the hypothesis that it belongs to the α-high component. Conversely, the locations of our α-high stars are 10 times more probable under the hypothesis that they belong to the α-high component than under the hypothesis that they belong to the α-low component. With this probabilistic separation criterion, we successfully determine separate kinematics for the α-low and -high populations, for a conservative metallicity range where a two-component model is plausible. In addition, we find cool, thin-disc-like kinematics for the majority of our sample above solar metallicity.

For the α-low sequence, we find a negative trend in the mean rotational velocity as a function of metallicity: $\partial V_\phi/\partial$[Fe/H] $= (-11 \pm 1)$ km s^{-1} dex^{-1}, which is a shallower gradient than those measured by high-resolution studies of the solar neighbourhood. For the α-high component, we find a positive correlation of mean rotational velocity with metallicity: $\partial V_\phi/\partial$[Fe/H] $= (51 \pm 10)$ km s^{-1} dex^{-1}, which agrees with results from both low- and high-resolution surveys.

Although a faint signature of this trend can be seen in the metal-rich bins of α-high sequence (open symbols in panel d of Fig. 4), we note that this may be due to contamination by α-low stars arising from the large errors in [Fe/H]. Also at the high-[Fe/H] end we notice a relative overabundance of α-high stars. A similar population of α-high, metal-rich stars was detected by Gazzano et al. (2013), who concluded that these objects probably belong to the thin disc. By contrast, Masseron & Gilmore (2015) consider it uncertain whether these stars should be assigned to the thin or thick disc on the grounds that these stars may have a variety of origins. Furthermore, it is possible that some of these α-high stars are young (Chiappini et al.

2015; Martig et al. 2015), which suggests that they are part of the thin disc (however, see Jofré et al. 2014 for a discussion on the existence of this population). For these reasons, we do not consider the kinematics of the SMR ([Fe/H] $\gtrsim 0.15$) stars in the α-high component.

The α-low and α-high components follow different trends for all three components of the velocity dispersion. While the velocity dispersions of the chemical disc components are similar in the metallicity regime $-0.2 <$ [Fe/H] < 0.0, there are significant differences at the metal-poor end. The mean dispersion of a given velocity component is $\sim$16 km s^{-1} less for α-low stars than α-high stars. Notwithstanding some contamination of one component by the other, our chemically separated components exhibit markedly different kinematics, which are consistent with the trends found using higher resolution data.

RAVE offers a unique statistical opportunity to constrain theories of Galaxy evolution. While high-resolution surveys will have a very small overlap with *Gaia* DR1, $\sim 3 \times 10^5$ RAVE stars are expected to be in *Gaia* DR1. Hence, RAVE data combined with more accurate parallaxes and proper motions from *Gaia* DR1 should significantly sharpen, and hopefully confirm, the chemodynamical trends reported here and enable us to track more securely the extent and effect of radial migration in the Galactic discs.

ACKNOWLEDGEMENTS

We thank the referee for their thorough comments and suggestions which have helped improve the quality of the manuscript. We also thank Philipp Richter, Ivan Minchev, Friedrich Anders, Cristina Chiappini, and Else Starkenburg for their comments and helpful discussions, which have improved the quality and clarity of the text. Funding for this work and for RAVE has been provided by the Australian Astronomical Observatory; the Leibniz-Institut fuer Astrophysik Potsdam (AIP); the Australian National University; the Australian Research Council; the European Research Council under the European Union's Seventh Framework Programme (Grant Agreement 240271 and 321067); the French National Research Agency; the German Research Foundation (SPP 1177 and SFB 881); the Istituto Nazionale di Astrosica at Padova; the Johns Hopkins University; the National Science Foundation of the USA (AST-0908326); the W. M. Keck foundation; the Macquarie University; the Netherlands Research School for Astronomy; the Natural Sciences and Engineering Research Council of Canada; the Slovenian Research Agency; the Swiss National Science Foundation; the Science & Technology Facilities Council of the UK; Opticon; Strasbourg Observatory; and the Universities of Groningen, Heidelberg and Sydney. The RAVE website is https://www.rave-survey.org.

REFERENCES

Adibekyan V. Z. et al., 2013, A&A, 554, A44
Aumer M., Binney J. J., 2009, MNRAS, 397, 1286
Aumer M., Binney J., Schönrich R., 2016, MNRAS, 459, 3326
Bensby T., Feltzing S., Lundström I., 2003, A&A, 410, 527
Bensby T., Feltzing S., Lundström I., Ilyin I., 2005, A&A, 433, 185
Bensby T., Alves-Brito A., Oey M. S., Yong D., Meléndez J., 2011, ApJ, 735, L46
Bensby T., Feltzing S., Oey M. S., 2014, A&A, 562, A71
Bergemann M. et al., 2014, A&A, 565, A89
Bertelli G., Girardi L., Marigo P., Nasi E., 2008, A&A, 484, 815
Binney J. et al., 2014a, MNRAS, 437, 351
Binney J. et al., 2014b, MNRAS, 439, 1231
Bland-Hawthorn J., Gerhard O., 2016, preprint (arXiv:1602.07702)
Boeche C. et al., 2011, AJ, 142, 193
Boeche C. et al., 2013, A&A, 559, A59
Bournaud F., Elmegreen B. G., Martig M., 2009, ApJ, 707, L1
Bovy J., Rix H.-W., Hogg D. W., 2012a, ApJ, 751, 131
Bovy J., Rix H.-W., Liu C., Hogg D. W., Beers T. C., Lee Y. S., 2012b, ApJ, 753, 148
Bovy J., Bird J. C., García Pérez A. E., Majewski S. R., Nidever D. L., Zasowski G., 2015, ApJ, 800, 83
Brook C. B., Kawata D., Gibson B. K., Freeman K. C., 2004, ApJ, 612, 894
Cartledge S. I. B., Lauroesch J. T., Meyer D. M., Sofia U. J., 2006, ApJ, 641, 327
Chen B. et al., 2001, ApJ, 553, 184
Chiappini C., Matteucci F., Gratton R., 1997, ApJ, 477, 765
Chiappini C. et al., 2015, A&A, 576, L12
Chiba M., Beers T. C., 2000, AJ, 119, 2843
De Silva G. M. et al., 2015, MNRAS, 449, 2604
Edvardsson B., Andersen J., Gustafsson B., Lambert D. L., Nissen P. E., Tomkin J., 1993, A&A, 275, 101
Freeman K., Bland-Hawthorn J., 2002, ARA&A, 40, 487
Fuhrmann K., 1998, A&A, 338, 161
Fuhrmann K., 2004, Astron. Nachr., 325, 3
Fuhrmann K., 2008, MNRAS, 384, 173
Fuhrmann K., 2011, MNRAS, 414, 2893
Gazzano J.-C., Kordopatis G., Deleuil M., de Laverny P., Recio-Blanco A., Hill V., 2013, A&A, 550, A125
Genovali K. et al., 2014, A&A, 566, A37
Gilmore G., Wyse R. F. G., Kuijken K., 1989, ARA&A, 27, 555
Gilmore G. et al., 2012, The Messenger, 147, 25
Golubov O. et al., 2013, A&A, 557, A92
Grenon M., 1972, in Cayrel de Strobel G., Delplace A. M., eds, IAU Colloq. 17: Age des Etoiles. Paris, France, p. 55
Guiglion G. et al., 2015, A&A, 583, A91
Hayden M. R. et al., 2015, ApJ, 808, 132
Haywood M., 2008, MNRAS, 388, 1175
Haywood M., Di Matteo P., Lehnert M. D., Katz D., Gómez A., 2013, A&A, 560, A109
Haywood M., Lehnert M. D., Di Matteo P., Snaith O., Schultheis M., Katz D., Gomez A., 2016, A&A, 589, A66
Holmberg J., Nordström B., Andersen J., 2007, A&A, 475, 519
Israelian G., Meynet G., eds, 2008, The Metal-Rich Universe. Cambridge Univ. Press, Cambridge
Jofré P. et al., 2014, A&A, 564, A133
Jurić M. et al., 2008, ApJ, 673, 864
Just A., Jahreiß H., 2010, MNRAS, 402, 461
Kordopatis G. et al., 2011, A&A, 535, A107
Kordopatis G. et al., 2013, AJ, 146, 134 (K13)
Kordopatis G. et al., 2015a, MNRAS, 447, 3526
Kordopatis G. et al., 2015b, A&A, 582, A122
Lee Y. S. et al., 2011, ApJ, 738, 187
Lindegren L., Feltzing S., 2013, A&A, 553, A94
Loebman S. R., Roškar R., Debattista V. P., Ivezić Ž., Quinn T. R., Wadsley J., 2011, ApJ, 737, 8
Majewski S. R. et al., 2015, preprint (arXiv:1509.05420)
Martig M. et al., 2015, MNRAS, 451, 2230
Masseron T., Gilmore G., 2015, MNRAS, 453, 1855
Matijevič G. et al., 2012, ApJS, 200, 14
Minchev I., Famaey B., Quillen A. C., Dehnen W., Martig M., Siebert A., 2012, A&A, 548, A127
Minchev I., Chiappini C., Martig M., 2013, A&A, 558, A9
Monari G., Helmi A., Antoja T., Steinmetz M., 2014, A&A, 569, A69
Nidever D. L. et al., 2014, ApJ, 796, 38
Nissen P. E., Schuster W. J., 2010, A&A, 511, L10
Nordström B. et al., 2004, A&A, 418, 989
Pasetto S. et al., 2012, A&A, 547, A71
Piffl T. et al., 2014, A&A, 562, A91

Quillen A. C., Garnett D. R., 2001, in Funes J. G., Corsini E. M., eds, ASP Conf. Ser. Vol. 230, Galaxy Disks and Disk Galaxies. Astron. Soc. Pac., San Francisco, p. 87
Recio-Blanco A. et al., 2014, A&A, 567, A5
Reddy B. E., Lambert D. L., Allende Prieto C., 2006, MNRAS, 367, 1329
Richter P., 2006, in Roeser S., ed., Reviews in Modern Astronomy, Vol. 19. Wiley-VCH Verlag, Weinheim, Germany, p. 31
Richter P., Sembach K. R., Wakker B. P., Savage B. D., Tripp T. M., Murphy E. M., Kalberla P. M. W., Jenkins E. B., 2001, ApJ, 559, 318
Robin A. C., Reylé C., Derrière S., Picaud S., 2003, A&A, 409, 523
Roeser S., Demleitner M., Schilbach E., 2010, AJ, 139, 2440
Schönrich R., 2012, MNRAS, 427, 274
Schönrich R., Binney J., 2009a, MNRAS, 396, 203
Schönrich R., Binney J., 2009b, MNRAS, 399, 1145
Schönrich R., Binney J., Dehnen W., 2010, MNRAS, 403, 1829
Sellwood J. A., Binney J. J., 2002, MNRAS, 336, 785
Siebert A. et al., 2008, MNRAS, 391, 793
Siebert A. et al., 2011, MNRAS, 412, 2026
Skrutskie M. F. et al., 2006, AJ, 131, 1163
Soubiran C., Bienaymé O., Siebert A., 2003, A&A, 398, 141
Steinmetz M. et al., 2006, AJ, 132, 1645
Vickers J. J., Roeser S., Grebel E. K., 2016, AJ, 151, 99
Wakker B. P., 2001, ApJS, 136, 463
Williams M. E. K. et al., 2013, MNRAS, 436, 101
Yanny B. et al., 2009, AJ, 137, 4377
Zacharias N., Finch C. T., Girard T. M., Henden A., Bartlett J. L., Monet D. G., Zacharias M. I., 2013, AJ, 145, 44
Žerjal M. et al., 2013, ApJ, 776, 127
Zhao G., Zhao Y.-H., Chu Y.-Q., Jing Y.-P., Deng L.-C., 2012, Res. Astron. Astrophys., 12, 723

This paper has been typeset from a TEX/LATEX file prepared by the author.